



PERGAMON

Available online at www.sciencedirect.com

SCIENCE @ DIRECT®

Polyhedron 22 (2003) 1755–1758



POLYHEDRON

www.elsevier.com/locate/poly

Weak-ferromagnetism in molecular magnets based on transition metal complexes of crown thioether

Junichi Nishijo*, Akira Miyazaki, Toshiaki Enoki*

Department of Chemistry, Graduate School of Science and Engineering, Tokyo Institute of Technology, Ookayama, Meguro-ku, Tokyo 152-8551, Japan

Received 6 October 2002; accepted 12 December 2002

Abstract

A new class of molecular based magnets $M(9S3)_2[Ni(bdt)_2]_2$ ($M = Ni, Co$) consisting of transition metal complex of crown thioether show weak-ferromagnetic transitions at $T_N = 6.2$ and 2.6 K for $M = Ni$ and Co , respectively, accompanied by remanent magnetizations $0.2\mu_B$ and $0.01\mu_B$ with coercive forces 200 and 10 Oe. $M(9S3)_2^{2+}$ cations ($S = 1$ and $1/2$ for $M = Ni$ and Co , respectively), and a half of $Ni(bdt)_2^-$ ($S = 1/2$) anions form alternate antiferromagnetic (AF) chains (#1), while the other half of $Ni(bdt)_2^-$ anions form uniform AF chains (#2). These two type of chains are connected to each other by two weak AF interactions; interaction between $Ni(bdt)_2^-$ in #1 and $Ni(bdt)_2^-$ in #2, and interaction between $M(9S3)_2^{2+}$ in #1 and $Ni(bdt)_2^-$ in the adjacent chain #1. A competition between these two AF interactions causes canted spin configuration, giving rise to weak-ferromagnetism. © 2003 Elsevier Science Ltd. All rights reserved.

Keywords: Weak-ferromagnetism; Ferrimagnet; Molecular based magnet; Transition metal complex; Crown thioether; Benzene dithiolate

1. Introduction

Transition metal complexes of dithiolate are of particular interests in designing molecular-based magnets. Inter-molecular magnetic interaction owing to its planar molecular shape makes the magnetic system low dimensional [1,2], and occasionally it causes ferromagnetic interactions depending of the molecular packing manner [2–5]. In addition, sulfur atoms present in the molecule work to give strong magnetic interaction through the formation of inter-molecular sulfur–sulfur short contacts between ligands or sulfur–transition metal contacts. To enhance such inter-molecular magnetic interactions, transition metal-incorporated crown thioether is a promising cation molecule to be effectively connected to dithiolate through sulfur–sulfur bridging superexchange paths. In the present paper, we report a new class of molecular based magnets $M(9S3)_2[Ni(bdt)_2]_2$ ($M = Ni, Co$; $9S3 = 1,4,7$ -trithiacyclononane,

$bdt = benzenedithiolate$) which consist of dithiolate planar complex $Ni(bdt)_2^-$ as $S = 1/2$ anion and crown thioether complex $M(9S3)_2^{2+}$ as $S = 1$ ($M = Ni$) or $S = 1/2$ ($M = Co$) cation (Fig. 1).

2. Experimental

$M(9S3)_2(BF_4)_2$ and $TBA_2Ni(bdt)_2$ were prepared according to the published methods [6,7]. Fifty milliliter acetonitrile solution of 50 mg $M(9S3)_2(BF_4)_2$ was added to 50 ml acetonitrile solution of 50 mg $TBA_2Ni(bdt)_2$, and the mixture was cooled to $0^\circ C$. After standing for 4 h at the temperature, black elongated plate crystals of $M(9S3)_2[Ni(bdt)_2]_2$ were obtained, whose typical crystal size is $3 \times 1 \times 0.1$ mm. The crystal structures are determined by single crystal X-ray diffraction method with *Rigaku* AFC-7 four-circle diffractometer at 293 K, using Mo K α radiation, on suitable crystal mounted on glass fiber. Structure were solved using direct methods (SHELXS-86) [8], then refined with full-matrix least-squares method (SHELXL-93) [9]. Magnetic susceptibilities were measured by using Quantum-Design MPMS-5 SQUID magnetometer for one single crystalline sample

* Corresponding author. Tel.: +81-3-5734-2610; fax: +81-3-5734-2242.

E-mail addresses: jnishijo@chem.titech.ac.jp (J. Nishijo), tenoki@chem.titech.ac.jp (T. Enoki).

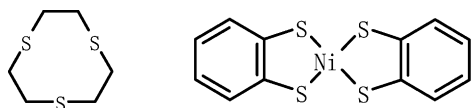


Fig. 1. Molecular structures of 9S3 (left) and $\text{Ni}(\text{bdt})_2^-$ (right).

whose typical size and weight are $5 \times 2 \times 0.1$ mm and 1.5 mg, respectively.

3. Results and discussion

$\text{M}(\text{9S3})_2[\text{Ni}(\text{bdt})_2]_2$ ($\text{M} = \text{Ni}, \text{Co}$) are isostructural as depicted in Fig. 2, where an $\text{M}(\text{9S3})_2^{2+}$ molecule with surrounding four $\text{Ni}(\text{bdt})_2^-$ molecules constitutes a cage-like unit. The network of cage-like units forms a plane extended along the $a+c$ and $b+c$ directions (Fig. 2(a)), while these planes are stacked in a slip-faced manner in the c -axis direction; $\text{M}(\text{9S3})_2^{2+}$ being located just above the $\text{Ni}(\text{bdt})_2^-$ of the lower plane (Fig. 2(b)). From the viewpoint of magnetic structure, inter-molecular short contacts, especially S–S contacts, are important for the formation of superexchange paths. In the present crystals, it is expected that there are two strong superexchange interaction paths J_A and J_C

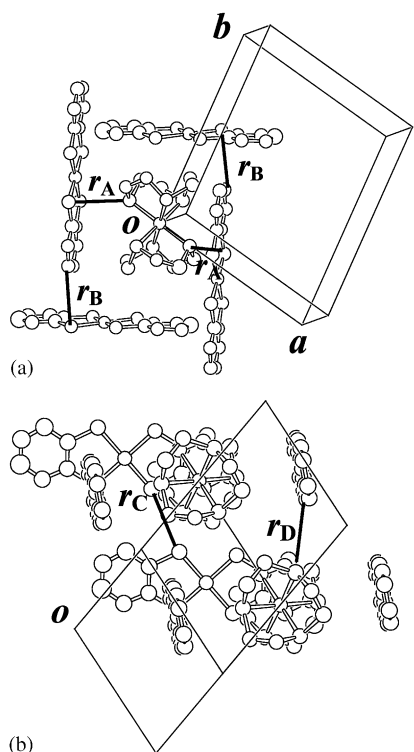


Fig. 2. Crystal structure of $\text{M}(\text{9S3})_2[\text{Ni}(\text{bdt})_2]_2$ ($\text{M} = \text{Ni}, \text{Co}$). (a) Planar-shaped cage-like structure on the $(a+c)$ – $(b+c)$ plane and (b) stacking of the cage-like structure along the c -axis. $r_A = 3.77$ Å and $r_D = 3.98$ Å, respectively, are short S–S and short CH–S contacts between $\text{M}(\text{9S3})_2^{2+}$ and $\text{Ni}(\text{bdt})_2^-$. $r_B = 3.75$ Å and $r_C = 3.78$ Å are short CH–S and short S–S contacts between $\text{Ni}(\text{bdt})_2^-$ molecules, respectively.

through short S–S contacts ($r_A = 3.77$ Å and $r_C = 3.78$ Å, respectively), whose distances are roughly equal to the sum of van der Waals radii (3.70 Å). In addition to these strong interaction paths, two weak interaction paths J_B and J_D are produced by CH–S contacts ($r_B = 3.75$ Å and $r_D = 3.98$ Å, respectively), which are somewhat longer than the sum of van der Waals radii (3.55 Å). Judging from a comparison of the path lengths, J_A and J_C have roughly same value, and J_B is stronger than J_D . Furthermore, J_A and J_C are stronger than J_B and J_D ; $|J_A|, |J_C| \gg |J_B| > |J_D|$. Therefore, the magnetic structure consists of two kinds of chains weakly interacting with each other. $\text{M}(\text{9S3})_2^{2+}$ cations and a half of $\text{Ni}(\text{bdt})_2^-$ anions form alternate antiferromagnetic (AF) chains #1 spanned by J_A along the $a+c$ direction, while the other half of $\text{Ni}(\text{bdt})_2^-$ anions connected by J_C form uniform AF chains #2 along the c direction. These two magnetic chains are weakly bound to each others by AF path J_B between $\text{Ni}(\text{bdt})_2^-$ anions of #1 and #2 chains, and in addition, adjacent chains #1 are directly bound to each other by weak AF interaction J_D between $\text{Ni}(\text{bdt})_2^-$ and $\text{M}(\text{9S3})_2^{2+}$.

Fig. 3 shows the temperature dependence of magnetic susceptibility of $\text{Ni}(\text{9S3})_2[\text{Ni}(\text{bdt})_2]_2$ in the fields applied in three independent directions after the subtraction of the core diamagnetic contribution. The susceptibility χ obeys the Curie–Weiss law with negative Weiss temperature $\theta = -6.5$ K and Curie constant $C = 1.76$ emu K mol $^{-1}$, the latter of which corresponds to one $S = 1$ spin of $\text{Ni}(\text{9S3})_2^{2+}$ and two $S = 1/2$ spins of $\text{Ni}(\text{bdt})_2^-$ per formula unit. χ increases more steeply than that expected from the Curie–Weiss law as the temperature is lowered in the temperature range of $6 < T < 8$ K when the external field H is applied parallel to the x and y directions. In the Ni salt, chains #1, which are the alternate AF chains of $S = 1$ and $S = 1/2$, are expected to behave as ferrimagnetic (FI) chains with strong intra-chain AF interaction J_A , under the weak internal field produced by inter-chain interactions J_D between adjacent chains #1 and J_B between chain #1 and chain #2.

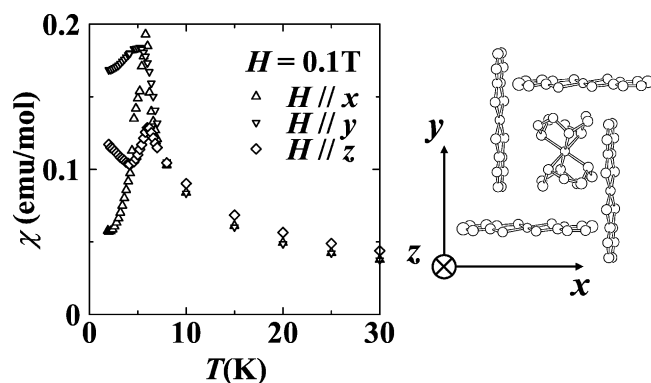


Fig. 3. Magnetic susceptibility of $\text{Ni}(\text{9S3})_2[\text{Ni}(\text{bdt})_2]_2$ in the fields 0.1 T applied along three independent directions x , y and z . The directions are defined in the right figure.

Therefore, the FI chain #1 is considered to be responsible for the steep increase of the susceptibilities. The fact that the steep increase is observed only in $H \parallel x$ and $H \parallel y$ suggests the feature of XY spin anisotropy of the FI chains #1. This anisotropy, however, is weak because the difference of χ between $H \perp z$ and $H \parallel z$ is observed only in the low temperature region below approximately 8 K. After the steep increase in the susceptibility, an AF transition takes place at $T_N = 6.2$ K, as evidenced by the appearance of susceptibility peaks for all the field directions. Fig. 4 shows the magnetization curves at $T = 2$ K. Below T_N , the magnetization curve of $H \parallel y$ shows a hysteresis loop with a discontinuous change at coercive force $H_C = 200$ Oe and a remanent magnetization $M_{REM} = 0.2\mu_B$, which is the evidence of weak-ferromagnetism. A spin flop is observed at approximately 1.7 T in $H \parallel x$, while χ steeply approaches zero as the temperature goes to 0 K only in this direction. This suggests that the easy axis is oriented to the x direction.

In the case of the Co salt, the susceptibility also obeys the Curie–Weiss law with Weiss temperature $\Theta = -2.3$ K and Curie constant $C = 1.21$ emu K mol⁻¹, the latter of which corresponds to three $S = 1/2$ spins of $Ni(9S3)_2^{2+}$ and $Ni(bdt)_2^-$ per formula unit. Different from the Ni salt, the chain #1 of the Co salt consists of only $S = 1/2$ spins, resulting in the absence of FI structure. Reflecting this magnetic feature, no conspicuous increasing of the susceptibilities in $H \parallel x$ and $H \parallel y$ is observed just above $T_N = 2.6$ K. Below T_N , the Co salt also shows weak-ferromagnetism with $M_{REM} = 0.02\mu_B$ and $H_C = 10$ Oe, which are one order of magnitude smaller than those of the Ni counterpart. Substituting Co ($S = 1/2$) for Ni ($S = 1$) leads to the

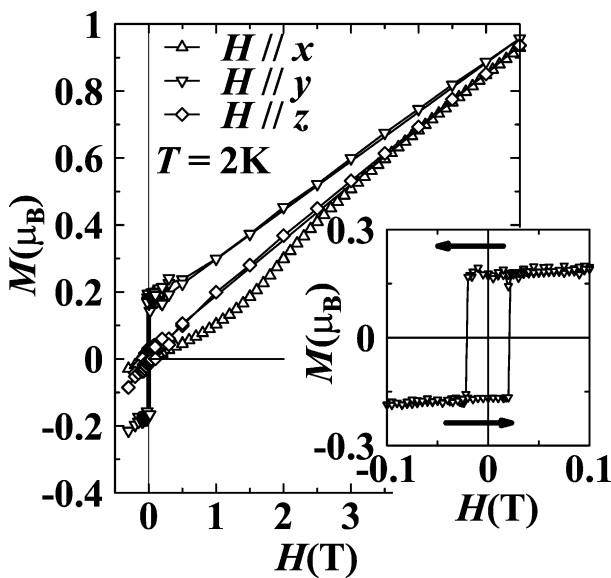


Fig. 4. Magnetization curves of $Ni(9S3)_2[Ni(bdt)_2]_2$ in the fields applied along the x , y and z directions. Inset is the enlargement of the low magnetic field region of $H \parallel y$.

disappearance of FI structure in the chain #1 and weakening of the inter-chain AF interaction between the chains #1 (J_D). Therefore, such a large difference in the weak-ferromagnetism between the Ni and Co salts suggests that at least either FI structure or the AF interactions J_D between chains #1 plays an important role in the origin of the weak-ferromagnetism.

Here, we discuss the origin of the weak-ferromagnetism. There are several candidates for the origin. However, among these, Dzyaloshinskii–Moriya interaction is excluded from the origin in the present case because of the presence of inversion center. Single ion anisotropy is also not a candidate. The absence of a spontaneous magnetization associated with the FI chains #1 in the Ni salt below T_N indicates antiparallel arrangement between the adjacent FI chains #1, resulting in the compensation of the single ion anisotropies of $Ni(9S3)_2^{2+}$ and $Ni(bdt)_2^-$ in chains #1. Similarly, single ion anisotropies of $Ni(bdt)_2^-$ anions in chains #2 are also compensated with the adjacent anions in the same chain #2. In contrast, a competition of two AF interactions J_B and J_D can be a candidate for the origin of the weak-ferromagnetism. In the Ni salt, the chains #1 along the $a+c$ direction are FI $S = 1$ and $S = 1/2$ alternate chains, and the chains #2 along the c -axis are uniform AF chains with $S = 1/2$. In the first step of the discussion, we take only J_A , J_B and J_C to consider a

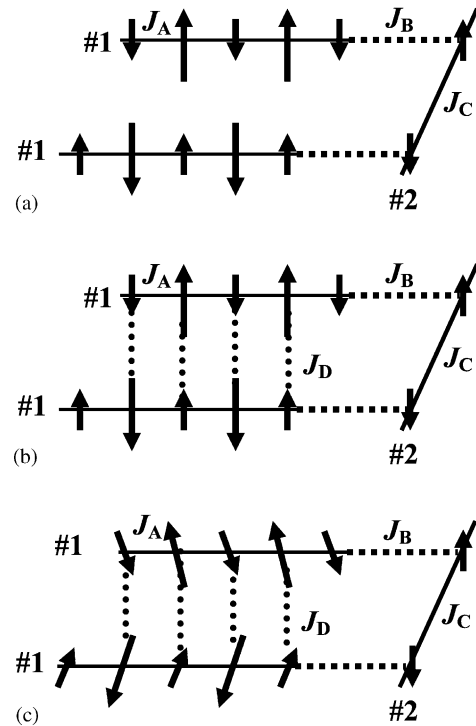


Fig. 5. (a) Magnetic structure model with three AF exchange interactions J_A , J_B and J_C ($|J_A|, |J_B| \gg |J_C|$). (b) Introducing the weak AF inter-chain interaction J_D destabilizes the spin configuration of (a). (c) Magnetic structure model with J_A , J_B , J_C and J_D , where spin frustration effect is reduced by canting of easy axes of chain #1.

possible spin structure, as shown in Fig. 5(a). In this structure, the FI chains #1 are connected in antiparallel to the AF chains #2 through J_B . For the next step, J_D , the weak inter-chain interaction between chains #1, is introduced to the magnetic structure model (Fig. 5(b)). The spin configuration of Fig. 5(b) has frustration because of the parallel spin configuration against AF interaction J_D . To reduce the energy caused by the spin frustration, the easy axes of the spins in the chains #1 are forced to cant (Fig. 5(c)). In the first approximation, the collinear structure in the chain #1 is assumed to be conserved against the inter-chain interactions because of strong intra-chain AF interaction J_A . This means that the spins of an FI chain cant to the same direction in concert with respect to the spins of the adjacent FI chain, giving rise to the generation of a spontaneous magnetic moment. In the Co salt, the spin canting of the chains #1 may also occur, but such a canting cannot cause spontaneous magnetization because the chain #1 has no net magnetic moment. One possible case of weak-ferromagnetism in the Co salt is the spin canting of the chains #2. Though J_C is quite stronger than J_B and J_D , the spin canting of chain #1 induces a small spin canting in the chain #2. Such a canting can also cause the weak-ferromagnetism in the Co salt. However, strong J_C allows only a very small canting angle. Furthermore, the weakening of the inter-chain interaction between the chains #1 caused by substituting $\text{Co}(\text{9S3})_2^{2+}$ ($S=1/2$) for $\text{Ni}(\text{9S3})_2^{2+}$ ($S=1$) tends to diminish the canting angle. Consequently, only quite weak weak-ferromagnetism was observed. Similar canting of the chain #2 also occurs in the Ni salt, but the weak-ferromagnetism of the Ni salt is governed by the canting in the chain #1, in addition to the weak canting in the chain #2.

4. Summary

$\text{M}(\text{9S3})_2[\text{Ni}(\text{bdt})_2]_2$ ($\text{M} = \text{Ni}, \text{Co}$) consists of two kinds of magnetic chains; alternate AF chain of $\text{M}(\text{9S3})_2^{2+}$ and $\text{Ni}(\text{bdt})_2^-$ spins (#1) and uniform $\text{Ni}(\text{bdt})_2^-$ chain (#2). In the Ni salt, chains #1 consisting of $S=1$ of $\text{Ni}(\text{9S3})_2^{2+}$ and $S=1/2$ of $\text{Ni}(\text{bdt})_2^-$ are FI, and a competition between the two inter-chain interactions causes a spin canting of the chain #1,

producing weak-ferromagnetism. In the Co salt, where FI structure is absent, weak-ferromagnetism is associated with only a small canting of the chain #2. The origin of the weak-ferromagnetism is the consequence of cooperation of multiple inter-chain interactions in concert.

5. Supplementary material

Crystallographic data for the structural analyses have been deposited with the Cambridge Crystallographic Data Centre, CCDC Nos. 198892 and 198893. Copies of this information may be obtained free of charge from The Director, CCDC, 12 Union Road, Cambridge, CB2 1EZ, UK (fax: +44-1223-336033; e-mail: deposit@ccdc.cam.ac.uk or www: <http://www.ccdc.cam.ac.uk>).

Acknowledgements

This work is supported by a Grant-in-Aid for Scientific Research No. 12046231 from the Ministry of Education, Science, Sport and Culture, Japan.

References

- [1] C.T. Vance, R.D. Bereman, J. Bordner, W.E. Hatfield, J.H. Helms, *Inorg. Chem.* 24 (1985) 2905.
- [2] M.L. Allan, A.T. Coomber, I.R. Marsden, J.H.F. Martens, R.H. Friend, *Synthetic Met.* 55–57 (1993) 3317.
- [3] A.T. Coomber, D. Beljonne, R.H. Friend, J.L. Brédas, A. Charlton, N. Robertson, A.E. Underhill, M. Kurmoo, P. Day, *Nature* 308 (1996) 144.
- [4] M. Uruichi, K. Yakushi, Y. Yamashita, J. Qin, *J. Mater. Chem.* 8 (1998) 141.
- [5] J. Nishijo, E. Ogura, J. Yamaura, A. Miyazaki, T. Enoki, T. Takano, Y. Kuwatani, M. Iyoda, *Solid State Commun.* 116 (2000) 661.
- [6] W.N. Setzer, C.A. Ogle, G.S. Wilson, R.S. Glass, *Inorg. Chem.* 22 (1983) 266.
- [7] M.J. Baker-Hawkes, E. Billig, H.B. Gray, *J. Am. Chem. Soc.* 88 (1966) 4870.
- [8] G.M. Sheldrick, *SHELXS86*, program for crystal structure determination, Univ. of Göttingen, Federal Republic of Germany, 1986.
- [9] G.M. Sheldrick, *SHELXL93*, program for refinement of crystal structures, Univ. of Göttingen, Federal Republic of Germany, 1993.